AIAA JOURNAL
Vol. 42, No. 8, August 2004

Prediction of Fatigue Crack Growth After Single Overload in an Aluminum Alloy

C. M. Manjunatha* and B. K. Parida†
National Aerospace Laboratories, Bangalore 560 017, India

An analytical method using crack driving force parameter ΔK^* was developed to account for the single overload interaction effects on the constant amplitude fatigue crack growth behavior in D16 (2024-T3 equivalent) aluminum alloy. Crack growth acceleration and retardation were accounted for by using residual stress intensity concept. Fatigue crack growth behavior was predicted using this method for a thin SE(T) specimen subjected to 1) constant amplitude load and 2) constant amplitude load interspersed with single tensile overloads at certain intervals of crack length. Fatigue crack growth tests were performed with these load sequences, and the experimental crack growth results obtained were compared with predictions made by use of the proposed analytical method. All of the fatigue crack growth tests were performed in a servohydraulic test machine. Crack length was measured by the traveling microscope/cellulose acetate replication method. A fairly good correlation was obtained between the experimental and predicted fatigue crack growth curves under the applied loading sequence.

Nomenclature

a	=	crack length
C_1	=	constant used in Paris equation
C_2	=	exponent used in Paris equation
C_3	=	cyclic fracture toughness
$\mathrm{d}a/\mathrm{d}N$	=	fatigue crack growth rate
K	=	stress intensity factor (SIF)
$K_{\max}$, $K_{\min}$	=	maximum and minimum SIFs
$(K_{\max})_{\text{eff}}$, $(K_{\min})_{\text{eff}}$	=	effective maximum and minimum SIFs
$K_{\max}^{\text{OL}}$	=	maximum SIF for the overload cycle
K_{op}	=	crack opening SIF
K_R	=	residual SIF
K_R^W	=	Willenborg residual SIF
L	=	specimen length
N_{expt}	=	number of cycles to failure from experiment
N_{pred}	=	predicted number of cycles to failure
R	=	stress ratio
R_L	=	ratio of σ_{UL} to σ_{OL}
$R_{\max}$	=	limiting maximum stress ratio
t	=	specimen thickness
W	=	specimen width
Z	=	plastic zone diameter under given load
Z_{app}	=	plastic zone diameter due to applied load
Z_{OL}	=	plastic zone diameter due to overload
α	=	plastic zone constraint factor
δa	=	crack length extension from the point of application of overload
Δa	=	crack length extension
ΔK	=	SIF range
ΔK_0	=	effective threshold SIF range
ΔK^+	=	positive part of $(K_{\max} - K_{\min})$
ΔK^*	=	effective crack driving force parameter, $(\Delta K^+ K_{\max})^{0.5}$
$(\Delta K^*)_{\text{eff}}$	=	effective ΔK^*
ΔK_{th}^*	=	threshold value of ΔK^*
σ	=	nominal stress
σ_{UL}, σ_{OL}	=	stress corresponding to underload and overload
σ_y	=	yield stress
ϕ	=	proportionality factor
ϕ_R, ϕ_A	=	proportionality factor for retardation and acceleration
Ψ	=	overload shutoff ratio

Received 22 February 2003; revision received 15 December 2003; accepted for publication 13 March 2004.

*Scientist, Structural Integrity Division.
†Senior Scientist, Structural Integrity Division; currently Senior Engineer, Foster–Miller, Inc., Waltham, MA 02451. Associate Fellow AIAA.

Introduction

THE damage tolerance concept is widely used in aircraft industry to ensure flight safety and to enhance the fatigue life of aircraft components beyond the original design life. Based on fracture mechanics principles, the number of flights or time in flight hours required for a fatigue crack to grow from a given initial size to a certain critical size is evaluated for this purpose. Quite often, these types of crack growth data are taken into account for scheduling of inspection intervals for aircraft structural components in service. Also, such fatigue crack growth curves derived under spectrum loading sequence for primary structural members of the airframe facilitate estimation of safe life extension period of aging airframes.

The general procedure for fatigue crack growth prediction under spectrum loading by cycle-by-cycle method involves the following steps: 1) experimental determination of material baseline constant amplitude fatigue crack growth rate (FCGR) data, 2) count (generally, rainflow cycle counting method) of fatigue load cycles in the spectrum load sequence, and 3) determination of crack length extension for each of these counted fatigue cycles from constant amplitude FCGR data with consideration of load sequence/interaction effects.

It is well established that constant amplitude FCGR can be represented as $\mathrm{d}a/\mathrm{d}N = f(\Delta K, R)$ (Ref. 1). Either Elber's crack closure concept[2] or two mechanical crack driving force parameters[3–8] ΔK and $K_{\max}$ are generally made use of to eliminate stress ratio R effects and obtain a characteristic single FCGR curve. Such a characteristic FCGR curve is approximated by a Paris (see Ref. 9) type of equation, $\mathrm{d}a/\mathrm{d}N = C[(\Delta K_{\text{eff}})$ or $f(\Delta K, K_{\max})]^m$, and is used subsequently for crack growth prediction under constant amplitude (CA) or spectrum loading.

Spectrum loading sequence, in its simplest form, consists of a CA load sequence interspersed with single overloads at frequent intervals of time. This type of load sequence is generally used as a baseline to analyze and develop crack growth models for load-interaction effects. Several authors have investigated fatigue crack growth behavior including single overload,[10–12] and many crack growth models have been developed to correlate experimental observations. These models can be broadly classified into those 1) based on the

crack closure concept[13–17] and 2) based on two mechanical driving forces,[17–21] ΔK and K_{max}.

In the methods based on crack closure concept, the crack driving force parameter ΔK is modified to ΔK_{eff}, to account for crack closure and stress ratio effects so that $da/dN = f(\Delta K_{eff})$ where $\Delta K_{eff} = K_{max} - K_{op}$. This procedure requires the experimental/numerical evaluation of crack opening stress intensity factor K_{op}. Careful experimental measurements have indicated that crack opening load P_{op} (and, hence, K_{op}) is not a unique value but depends on the measurement location and the technique employed.[22,23] Hertzberg et al.[24] found that the crack closure was only partially effective in explaining the observed crack growth behavior. Recently, Donald et al.[25] and Paris et al.[26] have shown that a significant contribution toward fatigue damage occurs in the load range even below the crack opening load. Meggiolaro et al.[13] found that crack closure cannot be used to explain the overload-induced retardation effects in their work and suggested to review the dominant role of crack closure on modeling crack growth. In spite of well-developed crack growth models for predictions, recently[16] there have been efforts to improve prediction accuracy by these models.

Furthermore, difficulties may be encountered for determination of fatigue crack closure level under spectrum loading, which is another required input parameter for accurate crack growth prediction. Under spectrum loading, closure level varies from cycle to cycle due to the varied nature of the variable amplitude load sequence.[1] Aircraft components are subjected to very many different types of spectrum loads, depending on the types of missions flown by the aircraft. Hence, experimental evaluation of fatigue crack closure level for each load cycle under such circumstances is practically impossible.

The other way of crack growth prediction is to ignore closure measurements altogether and acknowledge that the crack driving force is represented by two parameters,[8] ΔK and K_{max}. The load-interaction effect under overload is accounted for by considering plastic deformation ahead of the crack tip and its effect on altering the crack driving force parameters. Vasudevan et al.[3,27] argue that closure has limited effect on the fatigue damage process that takes place in front of the crack, whereas the crack closure phenomenon occurs behind the crack tip.

Recently, Kujawski[4] has used a crack driving force parameter ΔK^* [where $\Delta K^* = (\Delta K^+ K_{max})^{0.5}$, ΔK^+ is the value of the positive part of applied stress intensity factor (SIF) range, and K_{max} is the corresponding maximum value of the applied SIF] to account for effects of stress ratio in aluminum alloys. This ΔK^* (essentially a geometric mean of ΔK^+ and K_{max}) approach does not make use of any crack opening load/stress data. In Ref. 4, he has consolidated a vast amount of experimental data available in open literature for several aluminum alloys with stress ratios varying from $R = -1$ to $R = 0.7$ by use of ΔK^* as the effective crack driving force parameter. Analysis of fatigue crack growth under overloads using the ΔK^* approach appears to be quite simple because it eliminates evaluation of crack closure/opening load. However, applicability of the ΔK^* approach for crack growth prediction under overloads, which involves load-interaction effects, needs to be ascertained, and fatigue crack growth needs to be modeled.

In the present investigation, an analytical method using crack driving force parameter ΔK^* is developed to predict FCGR under constant amplitude load, including effects of single overload. Fatigue crack growth tests were performed under 1) CA load and 2) CA load interspersed with single overload at certain intervals of crack length. The experimental results were compared with crack growth predictions made by the described method.

Analytical Method

Fatigue Crack Growth

The crack driving force ΔK^* is defined as[4]

$$\Delta K^* = \left(\Delta K^+ K_{max}\right)^{0.5} \tag{1}$$

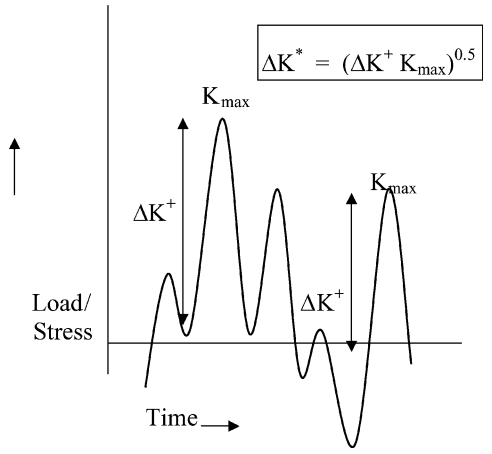

Fig. 1 Schematic representation of the crack driving force parameter ΔK^*.

where ΔK^+ is the value of the positive part of the applied SIF range and K_{max} is the corresponding maximum value of the applied SIF, as shown schematically in Fig. 1.

The fatigue crack growth rate da/dN is considered to be a function of the crack driving force parameter ΔK^* as $da/dN = f(\Delta K^*)$. This relationship can be expressed in the form of the Paris law (see Ref. 9) as $da/dN = C(\Delta K^*)^m$. However, This type of power law is inadequate at high growth rates approaching point of fracture,[28] as well as at low growth rates approaching threshold.[29] To account for the shortcomings, the complete sigmoidal shape of the FCGR curve is defined as

$$\frac{da}{dN} = C_1(\Delta K^*)^{C2}\left[1 - \left(\frac{\Delta K^*_{th}}{\Delta K^*}\right)^2\right] \Big/ \left[1 - \left(\frac{\Delta K^*}{C_3}\right)^2\right] \tag{2}$$

Note that Eq. (2) is similar in form to that proposed by Newman,[29] except for the following changes: 1) The term ΔK^* has been employed in place of ΔK_{eff} and K_{max}. 2) ΔK^*_{th} is used in place of ΔK_0. Use of ΔK^* in place of K_{max} has been necessitated in Eq. (2) because after representation of FCGR data in terms of ΔK^* the association of any given stress ratio with the specific experimental data is lost, and hence, K_{max} value can not be determined for any data in the resulting sigmoidal curve for use in Eq. (2). In this process, the present Eq. (2) uniquely defines the complete sigmoidal FCGR curve for any given material as a function of ΔK^*.

Overload Interaction Effects

Under the application of variable amplitude/spectrum load, various load interaction effects are present that affect fatigue crack growth behavior. A summary of the significant load interaction effects can be found elsewhere.[30] However, as a first step toward modeling the more complex fatigue crack growth behavior under spectrum load, the authors have concentrated in the present study only on the effect of single overload on fatigue crack growth behavior interspersed in a constant amplitude load sequence.

Consider imposition of a single-cycle tensile overload in a CA cyclic load sequence as shown in Fig. 2a. The effect of such a single tensile overload on fatigue crack growth behavior has been well established, and these effects have been modeled with crack closure consideration. A detailed summary of the load interactions observed under this type of loading can be found elsewhere.[11] Some of the major observations noted[11] are as follows:

1) The FCGR for the overload cycle is higher than that would be observed under CA loading with the same amplitude as that of the overload cycle. This has been termed crack growth acceleration.

2) The FCGRs for subsequent CA cycles after the application of single overload are lower than that which would be observed under CA loading with same cyclic load amplitude. This has been termed crack growth retardation.

3) The retardation effect of overload gradually decreases with increasing crack length and vanishes after a certain characteristic

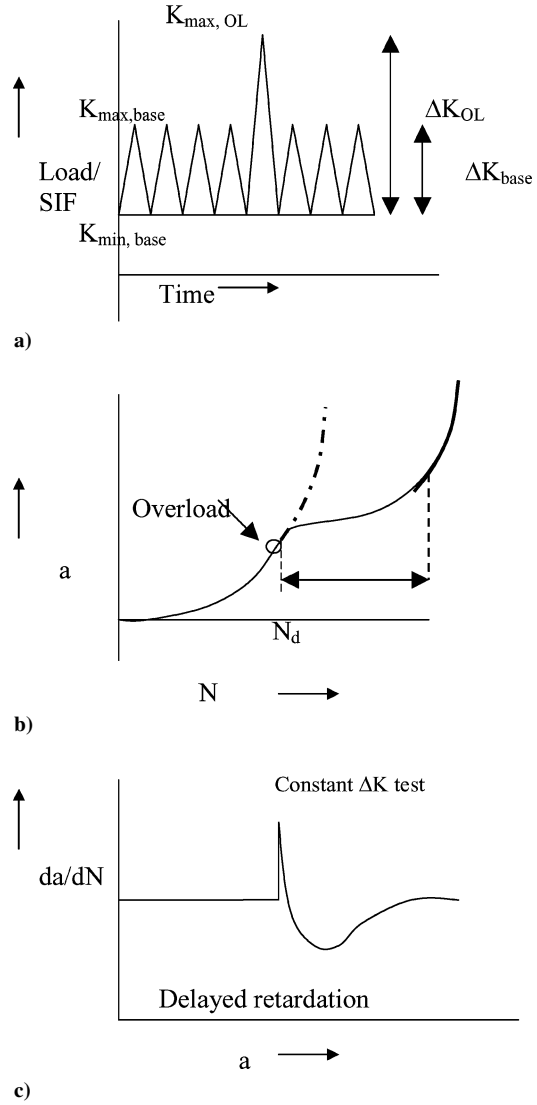

Fig. 2 Schematic of a) CA load interspersed with single-cycle tensile overload, b) corresponding fatigue crack growth, and c) delayed retardation due to tensile overload.

crack length extension from the position where overload cycle was applied. This characteristic distance has been modeled as either monotonic plastic zone radius[31] or plastic zone diameter.[32]

4) The maximum deceleration of growth rate occurs a short distance away from the point of application of overload. This effect has been termed delayed retardation.

All of these effects are schematically shown in Fig. 2. In the present method, the load interaction effects are calculated utilizing a residual stress intensity K_R concept.[32] Crack growth acceleration and retardation are accounted for by increasing or decreasing, respectively, the value of the crack driving force parameter ΔK^* to $(\Delta K^*)_{\text{eff}}$, that is,

$$(\Delta K^*)_{\text{eff}} = [\{(K_{\max})_{\text{eff}} - (K_{\min})_{\text{eff}}\}(K_{\max})_{\text{eff}}]^{0.5} \tag{3}$$

$$(K_{\max})_{\text{eff}} = K_{\max} - K_R \tag{4}$$

$$(K_{\min})_{\text{eff}} = K_{\min} - K_R \tag{5}$$

where K_R is the residual stress intensity factor, which will be defined subsequently. When K_R is positive, retardation occurs, and when it is negative, acceleration results. Note that, if $(K_{\min})_{\text{eff}} \leq 0$, then crack driving force parameter $(\Delta K^*)_{\text{eff}} = (K_{\max})_{\text{eff}}$.

The crack tip plastic zone associated with the application of a single overload interspersed in a constant amplitude load sequence is shown schematically in Fig. 3.

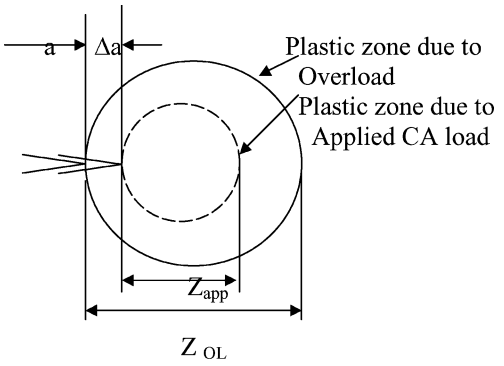

Fig. 3 Schematic of crack-tip plastic zone due to load cycles.

Possible load interaction effects[32] can be considered as follows:

$$\Delta a + Z_{\text{app}} = Z_{\text{OL}} \Rightarrow \text{no interaction effects} \tag{6}$$

$$\Delta a + Z_{\text{app}} < Z_{\text{OL}} \Rightarrow \text{crack growth retardation} \tag{7}$$

$$\Delta a + Z_{\text{app}} > Z_{\text{OL}} \Rightarrow \text{crack growth acceleration} \tag{8}$$

where Z is the plastic zone diameter at the crack tip and is given by

$$Z = [1/(\alpha\pi)](K_{\max}/\sigma_y)^2 \tag{9}$$

where $\alpha = 1.0$ for plane stress and $\alpha = 3.0$ for plain strain condition. The Willenborg et al. model[31] assumes Z_{OL} as the plastic zone radius, although retardation effects have been shown to last approximately one plastic zone diameter in some investigations.[33,34]

The residual stress intensity factor K_R [in Eqs. (4) and (5)] is obtained based on the generalized Willenborg et al.[31] model as suggested by Gallagher and Hughes[35]:

$$K_R = \Phi K_R^w \tag{10}$$

$$K_R^w = K_{\max}^{\text{OL}}(1 - \delta a/Z_{\text{OL}})^{0.5} - K_{\max} \tag{11}$$

where K_R^w is equal to the Willenborg et al. residual stress intensity factor, Φ is the proportionality factor[32,35] identical to acceleration (Φ_A) or retardation (Φ_R), which are given by

$$\Phi_A = 1 - R_L \tag{12}$$

$$R_L = \sigma_{\text{UL}}/\sigma_{\text{OL}} \tag{13}$$

$$\Phi_R = [1 - (K_{\text{th}}/K_{\max})]/(\Psi - 1) \tag{14}$$

where $\Psi = 2.3$ for aluminum alloys.[36] In the present context, after the unique material sigmoidal FCGR curve is obtained, K_{th} in Eq. (14) needs to be replaced with ΔK_{th}^* and Eq. (14) is rewritten as

$$\Phi_R = \left[1 - \left(\Delta K_{\text{th}}^* \middle/ K_{\max}\right)\right] \middle/ (\Psi - 1) \tag{15}$$

The Willenborg et al.[31] residual stress intensity factor K_R^w physically represents the difference between the stress intensity required to produce a current plastic zone equal to $(Z_{\text{OL}} - \Delta a)$ and the current applied maximum stress intensity $K_{\max}$. Hence, the statements made in Eqs. (6–8) can be restated in terms of K_R^w as 1) no interaction effect exists or there is no change in FCGR if K_R^w is zero, 2) crack growth rate retards if K_R^w is positive, and 3) it accelerates if K_R^w is negative.

The effect of overload on crack growth retardation reduces gradually with increase in crack length from the point of application of overload. This effect is reflected in Eq. (11). The variation of the term $[K_{\max}^{\text{OL}}(1 - \delta a/Z_{\text{OL}})^{0.5}]$ in Eq. (11) normalized with $K_{\max}^{\text{OL}}$, as a function $\delta a/Z_{\text{OL}}$ (crack length extension from the overload application point, normalized with overload plastic zone diameter) is schematically shown in Fig. 4.

It is assumed that the load interaction effects are active only up to a maximum stress ratio $R_{\max}$ above which $K_R = 0$ and, hence,

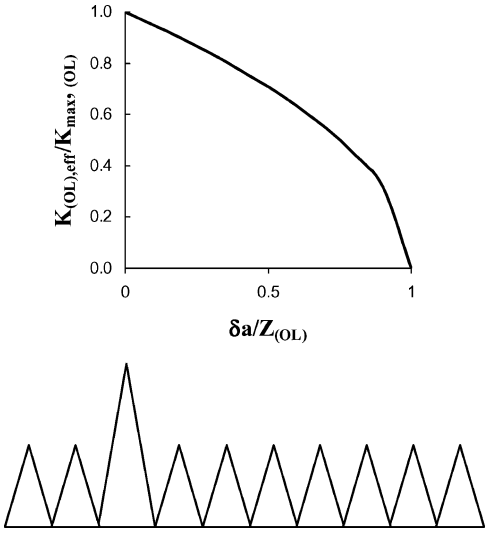

Fig. 4 Schematic representation of decay in retardation effect of tensile overload on subsequent CA load cycles.

$(\Delta K^*)_{\text{eff}} = \Delta K^*$. This $R_{\max}$ is considered to be a function of the constraints at the crack tip due to different stress states, that is, plane stress or plane strain. A simple relationship is used to determine the $R_{\max}$ as suggested by Johnson[32]:

$$R_{\max} = (Z/t)0.2 + 0.6 \tag{16}$$

Equation (16) suggests that for plain strain condition $Z/t \to 0$, hence, $R_{\max} = 0.6$. If the plastic zone diameter equals or exceeds the thickness, a state of plane stress condition is assumed and $R_{\max}$ is set to 0.8. The flow chart for fatigue crack growth prediction using described analytical model is shown in Fig. 5.

Experimental

Material and Specimen

The material used in this investigation was D16 (2024-T3 equivalent) aluminum alloy, which is mainly used in airframes. The standard chemical composition (in weight percent) of this material is as follows[37]: Cu 3.8–4.9, Mg 1.2–1.8, Mn 0.3–0.9, Si 0.5, Fe 0.5, Zn 0.3, and Al balance. The mechanical properties of the material determined from the tensile sheet specimens tested in longitudinal (LT) orientation were as follows: $\sigma_y = 347$ MPa, $\sigma_{\text{UTS}} = 460$ MPa, and percentage elongation = 12%.

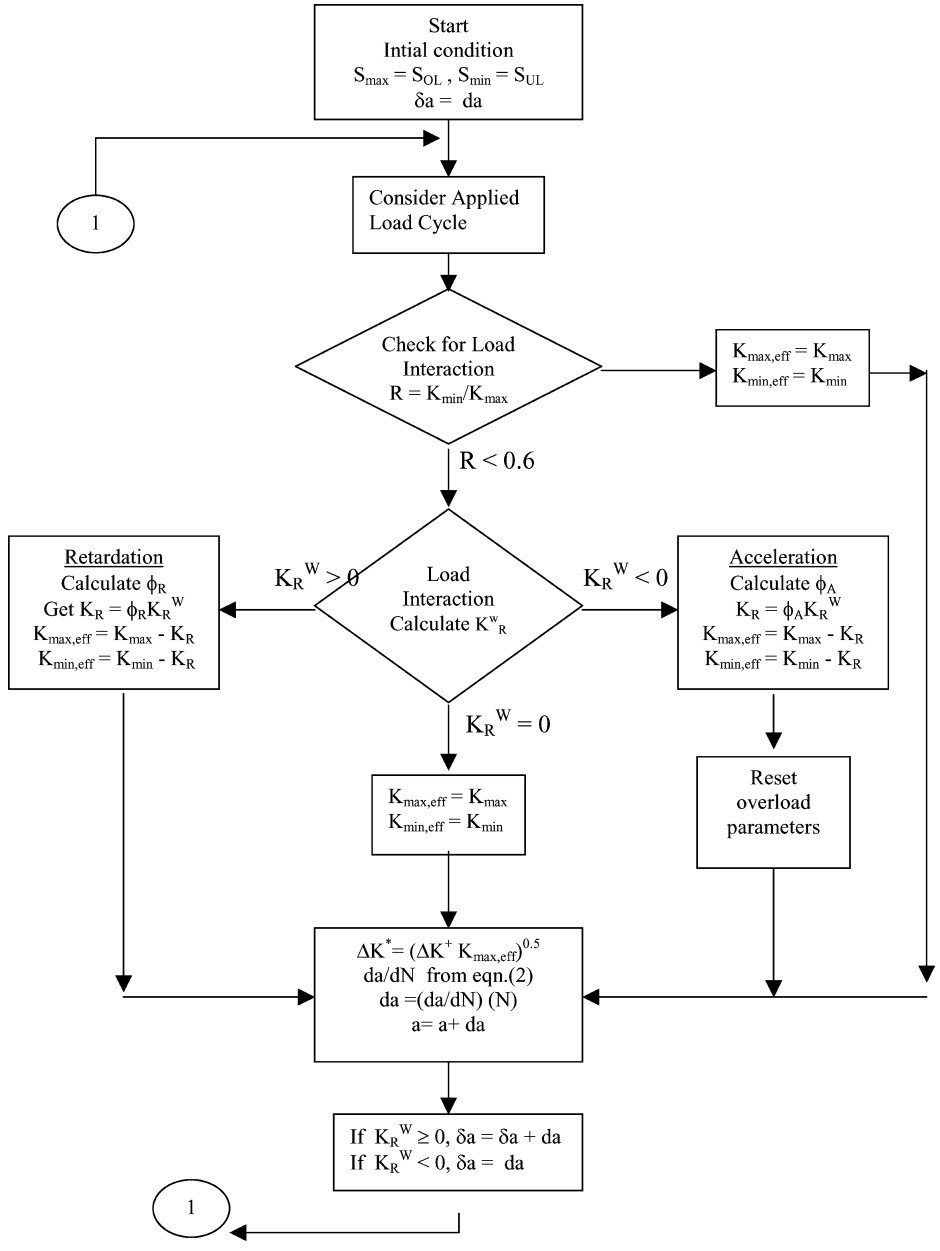

Fig. 5 Flowchart for the proposed analytical model to predict FCGR including tensile overload effects.

Fatigue crack growth tests were performed with a view to generate material FCGR data, using single-edge notched tension [SE(T)] specimens. Rectangular blanks were cut from the sheet material in LT orientation, and then these were finished to nominal dimensions of $W = 75$ mm, $L = 300$ mm, and $t = 1.5$ mm using a milling tool. A central U notch of length 3.5 mm and width 0.36 mm was cut on one edge of the specimen by wire electrical discharge machining (EDM). Specimens were buffed on both faces along the crack plane to facilitate crack length measurement.

Equipment and Procedure

Fatigue crack growth tests were performed in a computer-controlled, 100-kN, servohydraulic test machine. All of the tests were performed at room temperature and in laboratory air atmosphere. CA fatigue crack growth tests were performed as per American Society for Testing and Materials standard[38] E647 at different stress ratios ranging from $R = -0.3$ to $R = 0.7$ with a sinusoidal waveform at a frequency of 10 Hz.

Crack length was measured by the traveling microscope and/or cellulose acetate replication method. For measurement of crack length under the replication method, at any desired crack length the specimen was held at a small load of about 0.5 kN. The replication tape was dipped in acetone for a few seconds and then pressed on the cracked face of the specimen. It was then peeled off after drying and the replicas were observed in an optical microscope, which was attached to an image analysis system. The crack length was then measured accurately using the image analysis software.

For crack growth test involving compressive loads ($R = -0.3$), antibuckling guides were fixed on to the specimen during testing. The stress intensity factor K for a SE(T) specimen held inside hydraulic grips (uniform displacement condition) was calculated as[39]

$$K = f(a/W)\sigma\sqrt{(\pi a)} \tag{17}$$

where

$$f(a/W) = 5/[\{20 - 13(a/W) - 7(a/W)^2\}^{0.5}] \tag{18}$$

FCGR Test with and Without Overload

For comparison with predicted results, fatigue crack growth tests were performed using SE(T) specimens of D16 aluminum alloy subjected to CA cyclic loading with and without inserting single tensile overloads. The specimens with nominal dimensions of $W = 45$ mm, $L = 180$ mm, and $t = 1.5$ mm were precracked at $\sigma_{max} = 50$ MPa and $R = 0.1$ to a total crack length of about 4.0 mm. Then, baseline constant amplitude load cycles of $\sigma_{max} = 60$ MPa, $R = 0.1$ were applied, without inserting any overloads, and crack growth was carefully monitored until failure. A test was also performed with similar conditions but interspersed with single-cycle tensile overload of $\sigma_{max} = 120$ MPa, $\sigma_{min} = 6$ MPa ($R = 0.05$) at four different intervals of crack lengths. The overload cycle spacing was so chosen that the subsequent overload was applied only after the crack grew out of the plastic zone created by previous overload and had regained its original crack growth rate.

Results and Discussion

Baseline FCGR Results

To determine the crack growth law as in Eq. (2) for D16 aluminum alloy, CA fatigue crack growth tests were performed at different stress ratios, and the results obtained are shown in Fig. 6. Figure 6 is a conventional plot of crack growth rates da/dN as a function of applied SIF range ΔK. FCGRs were observed to increase with stress ratio R from -0.3 to 0.6. Crack growth rates at $R = 0.6$ and at $R = 0.7$ do not show significant difference. Similar effect of increasing growth rates with stress ratio R in aluminum alloys has been shown by various authors.[10,26,40–42]

The FCGRs da/dN from Fig. 6 were replotted in Fig. 7 as a function of crack driving force parameter ΔK^* [Eq. (1)]. The FCGR data were observed to merge into a narrow band, suggesting that the ΔK^* parameter provides a fairly good correlation with fatigue crack propagation rates in D16 aluminum alloy including stress ratio effects.

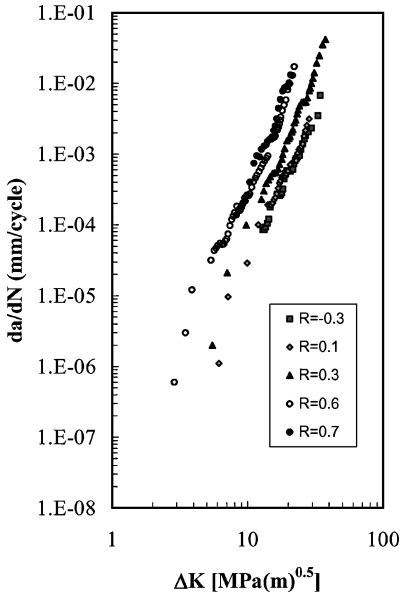

Fig. 6 Fatigue crack growth behavior of D16 aluminum alloy under CA loading.

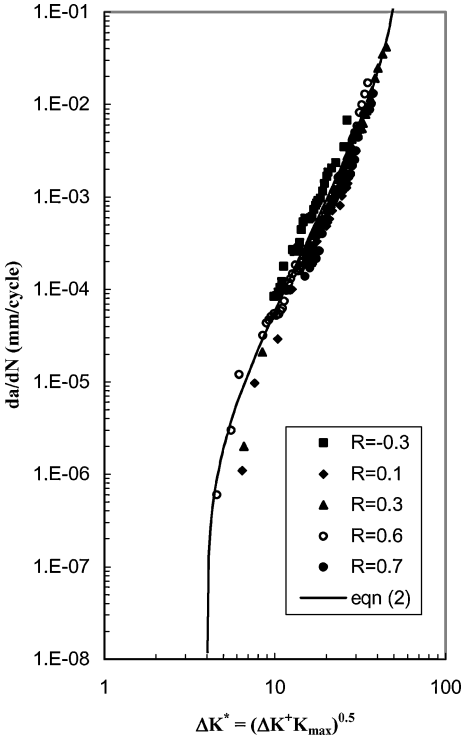

Fig. 7 FCGR expressed as a function of crack driving force parameter ΔK^*.

For the purpose of crack growth prediction under single overload condition, CA fatigue crack growth data shown in Fig. 7 were approximated in the form of Eq. (2). The constant C_3 representing cyclic fracture toughness of the material was taken as 55 MPa$\sqrt{}$m. $\Delta K^*_{th} = 4.0$ MPa $\sqrt{}$m, was obtained from the data in Fig. 7. The constants C_1 and C_2 were obtained by curve fitting to experimental data in Fig. 7. The numerical values of parameters determined are $C_1 = 1.7589\,e$-08 and $C_2 = 3.71$. When these parameters are used in Eq. (2), the predicted crack growth rate data for different values of ΔK^* are shown as a solid line in Fig. 7. As can be seen from Fig. 7, Eq. (2) with the given parameters describes the entire sigmoidal FCGR curve quite well.

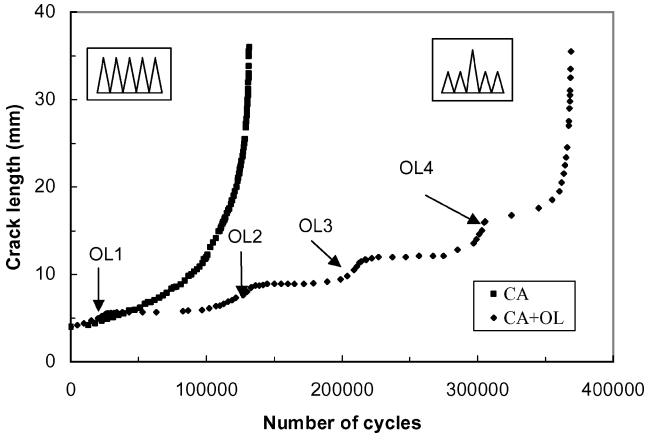

Fig. 8 Experimental results of fatigue crack growth under CA load and CA load interspersed with four single-cycle tensile overloads.

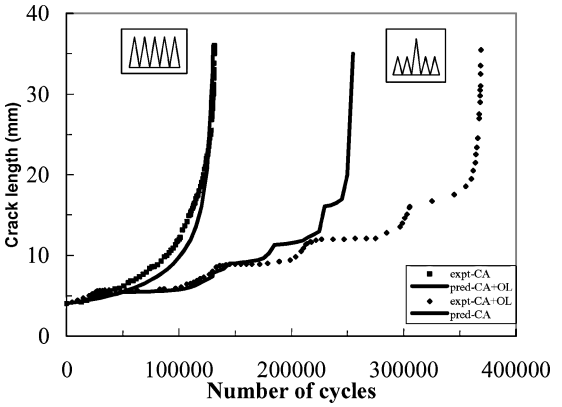

Fig. 9 Comparison of experimental and predicted fatigue crack growth behavior.

Fatigue Crack Growth Tests with and Without Overload Application

Fatigue crack growth tests were performed using SE(T) specimens of D16 aluminum alloy with and without application of overload. The details of the testing were explained earlier in the experimental section. Crack length extension as a function of fatigue cycles measured under CA loading with $\sigma_{max} = 60$ MPa, $R = 0.1$ (no overload) is shown in Fig. 8.

Fatigue crack growth results obtained under the same CA loading but interspersed with single-cycle tensile overload of $\sigma_{max} = 120$ MPa (twice the CA maximum stress of 60 MPa) at four different crack lengths are also shown in Fig. 8. The tensile overload effect of localized crack growth retardation can be clearly seen in Fig. 8. Similar crack growth retardation effects due to imposition of tensile overload cycles have been observed in 2024-T351 aluminum alloy by McMaster and smith.[16] In the present case, the total crack growth life was observed to increase by almost three times due to application of these four single overloads as shown in Fig. 8.

Fatigue Crack Growth Prediction

Fatigue crack growth in a thin SE(T) specimen of D16 (2024-T3 equivalent) aluminum alloy subjected to CA loading with and without application of single overload was predicted by the cycle-by-cycle method using the proposed analytical method explained earlier. Specimen dimensions taken were as follows: width = 45 mm and thickness = 1.43 mm (same as that of the test specimen). Initial crack length considered was $a = 4.0$ mm. The specimen was assumed to have been subjected to a CA load sequence with $\sigma_{max} = 60$ MPa, $\sigma_{min} = 6$ MPa, $R = 0.1$. To estimate fatigue crack growth, a computer program was developed that incorporated the logic explained in the flow chart shown in Fig. 5. The crack extension was computed for every load cycle considering 1) CA load with no overloads and 2) CA load interspersed with single overload applied at same crack lengths as in the experiment. The predicted results of fatigue crack growth obtained by using this analytical method along with the experimental results are shown in Fig. 9.

Fatigue crack growth behavior predicted by the method was observed to follow quite similar trends in relation to the experimentally observed behavior. Predicted total crack growth lives were found to be on the lower side of the experimental values under both no-overload and applied overload conditions, and hence, the predictions are conservative. The fatigue life ratios N_{expt}/N_{pred} were calculated to be 1.008 and 1.443, respectively for the earlier two cases. Achieving life ratios between 0.5 and 2.0 is generally considered as an excellent prediction of the total life results.[16]

Mcmaster et al.[16] investigated crack growth behavior in 2024-T351 aluminum alloy subjected to single overload and predicted the growth behavior using both constant and variable plastic constraint factors. A large scatter in life ratios, N_{expt}/N_{pred}, ranging from 0.93 to 3.69, was obtained for predictions using a constant constraint factor. However, use of a variable constraint factor lead to improvement in predictions with life ratios ranging from 0.95 to 2.04. In the present investigation, the fatigue life ratios range from 1.008 to 1.443 and appear to provide a fairly good correlation with experimental results. However, further experiments on fatigue crack growth under periodic overloads and underloads, as well as under spectrum load sequence, are required to validate the general applicability of the proposed method.

Conclusions

In this investigation, fatigue crack growth behavior in D16 (2024-T3 equivalent) aluminum alloy subjected to constant amplitude fatigue, including single overload cycles, was studied. An analytical method for prediction of crack growth under single overload, incorporating the crack driving force parameter ΔK^*, was proposed. The following conclusions may be drawn from the results obtained in this investigation:

1) Fatigue crack growth is retarded by application of single overload cycle during a CA fatigue test. The retardation effects disappear after a certain characteristic crack length extension from the overload position.

2) Fatigue crack growth behavior under single overload predicted by the proposed analytical method was able to account fairly well for load-interaction effects in D16 aluminum alloy considered in the present investigation.

3) The fatigue life ratios expressed as N_{expt}/N_{pred} were calculated to be 1.008 and 1.443 for the CA loading without and with overload application, respectively.

4) Further experiments on fatigue crack growth under different overload ratios and in various materials are necessary to investigate the applicability of the proposed analytical method for fatigue crack growth prediction.

Acknowledgments

The authors thank B.R. Pai, Director, National Aerospace Laboratories (NAL) for facilitating conduct of this research at the Structural Integrity Division, NAL. They also acknowledge with thanks assistance rendered by K. Sakthivel, M. Seshagirachari, K. Panbarasu, and G. Mani during the experimental part of this study.

References

[1]Schijve, J., "Prediction Methods for Fatigue Crack Growth in Aircraft Material," *Fracture Mechanics: Twelfth Conference*, ASTM STP 700, American Society for Testing and Materials, Philadelphia, 1980, pp. 3–34.

[2]Elber, W., "The Significance of Fatigue Crack Closure," *Damage Tolerance in Aircraft Structures*, ASTM STP 486, American Society for Testing and Materials, Philadelphia, 1971, pp. 230–242.

[3]Vasudevan, A. K., Sadananda, K., Louat, N., "A Review of Crack Closure, Fatigue Crack Threshold and Related Phenomena," *Materials Science and Engineering*, 1994, Vol. A188, pp. 1–22.

[4]Kujawski, D., "A New $(\Delta K^+ K_{max})^{0.5}$ Driving Force Parameter for Crack Growth in Aluminum Alloys," *International Journal of Fatigue*, Vol. 23, 2001, pp. 733–740.

[5]Kujawski, D., "A Fatigue Crack Driving Force Parameter with Load Ratio Effects," *International Journal of Fatigue*, Vol. 23, 2001, pp. S239–S246.

[6]Doker, H., "Fatigue Crack Growth Threshold: Implications, Determination and Data Evaluation," *International Journal of Fatigue*, Vol. 19, 1997, pp. S145–S149.

[7]Vasudevan, A. K., and Sadananda, K., "Classification of Fatigue Crack Growth Behavior," *Metallurgical and Materials Transcations*, Vol. 26A, 1995, pp. 1221–1234.

[8]Sadananda, K., and Vasudevan, A. K., "Crack Tip Driving Forces and Crack Growth Representation Under Fatigue," *International Journal of Fatigue*, Vol. 26, 2004, pp. 39–47.

[9]Paris, P. C., and Erdogan, F., "A Critical Analysis of Crack Propagation Laws," *Journal of Basic Engineering*, Vol. 85, 1963, pp. 528–534.

[10]Schijve, J., Skorupa, M., Skorupa, A., Machniewicz, T., and Gruszczynski, P., "Fatigue Crack Growth in the Aluminum Alloy D16 Under Constant and Variable Amplitude Loading," *International Journal of Fatigue*, Vol. 26, 2004, pp. 1–15.

[11]Sadananda, K., Vasudevan, A. K., Holtz, R. L., and Lee, E. U., "Analysis of Overload Effects and Related Phenomena," *International Journal of Fatigue*, Vol. 21, 1999, pp. S233–S246.

[12]Tur, Y. K., Vardar, O., "Periodic Tensile Overloads in 2024-T3 Alalloy", *Engineering Fracture Mechanics*, Vol. 53(1), 1996, pp. 69–77.

[13]Meggiolaro, M. A., and Pinho de Castro, J. T., "On the Dominant Role of Crack Closure on Fatigue Crack Growth Modeling," *International Journal of Fatigue*, Vol. 25, 2003, pp. 843–854.

[14]Voorwald, H. J. C., Torres, M. A. S., and Pinto Junoir, C. C. E., "Modelling of Fatigue Crack Growth Following Overloads," *International Journal of Fatigue*, Vol. 13, No. 5, 1991, pp. 423–427.

[15]Dexter, R. J., Hudak, S. J., Jr., and Davidson, D. L., "Modelling and Measurement of Crack Closure and Crack Growth Following Overloads and Underloads," *Engineering Fracture Mechanics*, Vol. 33, No. 6, 1989, pp. 855–870.

[16]McMaster, F. J., and Smith D. J., "Predictions of Fatigue Crack Growth in Aluminum Alloy 2024-T351 Using Constraint Factors," *International Journal of Fatigue*, Vol. 23, 2001, pp. S93–S101.

[17]Krenn, C. R., and Morris, J. R., Jr., "The Compatibility of Crack Closure And K_{max} Dependent Models of Fatigue Crack Growth," *International Journal of Fatigue*, Vol. 21, 1999, pp. S147–S155.

[18]Sheu B. C., Song, P. S., and Hwang, S., "Shaping Exponent in Wheeler Model Under a Single Overload," *Engineering Fracture Mechanics*, Vol. 51, No. 1, 1995, pp. 135–143.

[19]Lu, Y., and Li, K., "A New Model for Fatigue Crack Growth After a Single Overload," *Engineering Fracture Mechanics*, Vol. 46, No. 5, 1993, pp. 849–856.

[20]Arone, R., "Application of Wheeler Retardation Model for Assessment of Fatigue Crack Lifetime Under Random overloads," *International Journal of Fatigue*, Vol. 12, No. 4, 1990, pp. 275–281.

[21]Russell, S. G., "A New Model for Fatigue Crack Growth Retardation Following an Overload," *Engineering Fracture Mechanics*, Vol. 33, No. 6, 1995, pp. 839–854.

[22]Macha, D. E., Corby, D. M., and Jones, J. W., "On the Variation of Fatigue Crack Opening Load with Measurement Location," *Proceedings of the Society of Experimental Stress Analysis*, Vol. 36, Saugatuck Sta, Westport, CT, 1979, pp. 207–213.

[23]Shin, C. S., and Smith, R. A., "Fatigue Crack Growth from Sharp Notches," *International Journal of Fatigue*, Vol. 7, 1985, pp. 87–93.

[24]Hertzberg, R. W., Newton, C. H., and Jaccard, R., "Crack Closure: Correlation and Confusion," *Mechanics of Fatigue Crack Closure*, ASTM STP 982, American Society for Testing and Mateials, Philadelphia, 1988, pp. 139–148.

[25]Donald, K., and Paris, P. C., "An Evaluation of ΔK_{eff} Estimation Procedure on 6061-T6 and 2024-T3 Aluminum Alloys," *International Journal of Fatigue*, Vol. 21, 1999, pp. S47–S57.

[26]Paris, P. C., Tada, H., Donald, J. K., "Service Load Fatigue Damage—A Historical Perspective," *International Journal of Fatigue*, Vol. 21, 1999, pp. S35–S46.

[27]Vasudevan, A. K., Sadananda, K., and Louat, N., "Reconsideration of Fatigue Crack Closure," *Scripta Metallurgica et Materialia*, Vol. 27, 1992, pp. 1673–1678.

[28]Hardrath, H. F., Newman, J. C., Jr., Elber, W., and Poe, C. C., *Fracture Mechanics*, edited by N. Perrone, Univ. Press of Virginia, 1978, pp. 347–364.

[29]Newman, J. C., Jr., "A Crack-Closure Model for Predicting Fatigue Crack Growth Under Aircraft Spectrum Loading," *Methods and Models for Predicting Fatigue Crack Growth Under Random Loading*, ASTM STP 748, American Society for Testing and Materials, Philadelphia, 1981, pp. 53–84.

[30]Chang, J. B., "Round-Robin Crack Growth Predictions on Center-Cracked Tension Specimens Under Random Spectrum Loading," *Methods and Models for Predicting Fatigue Crack Growth*, ASTM STP 748, American Society for Testing and Materials, Philadelphia, 1981 pp. 3–40.

[31]Willenborg, J. D., Engle, R. M., Jr., and Wood, H. A., "A Crack Growth Retardation Model Using Effective Stress Concept," U.S. Air Force Flight Dynamics Lab., Rept. AFFDL-TM-71-1-FBR. Jan. 1971.

[32]Johnson, W. S., "Multi-parameter yield zone model for predicting spectrum crack growth," *Methods and Models for Predicting Fatigue Crack Growth*, ASTM STP 748, American Society for Testing and Materials, Philadelphia, 1981, pp. 85–102.

[33]Mill, W. J., Hertberg, R. W., and Roberts, R., *Cyclic Stress–Strain and Plastic Deformation Aspects of Fatigue Crack Growth*, ASTM STP 637, American Society for Testing and Materials, Philadelphia, 1977, pp. 192–208.

[34]Himmelein, M. K., and Hillberry, B. M., *Mechanics of Crack Growth*, ASTM STP 590, American Society for Testing and Mateials, Philadelphia, 1975, pp. 321–330.

[35]Gallagher, J. P., and Hughes, T. F., "Influence of Yield Strength on Overload Affected Fatigue Crack Growth Behavior in 4340 Steel," U.S. Air Force Flight Dynamics Lab., Rept. AFFDL-TR-74-27, July 1974.

[36]Probst, E. P., and Hillberry, B. M., "Fatigue Crack Delay and Arrest Due to Single Peak Tensile Overload," AIAA Paper 73-325, March 1973.

[37]Kurian, P. K., Chatterji, B., and Unnikrishnan, V., Foundry and Forge Div., (eds.), *Metallic Materials Data Book: Aerospace Applications*, Central Lab., Hindustan Aeronautics, Ltd., Bangalore, India, 1981.

[38]*Annual Book of ASTM Standards*, American Society for Testing and Materials, Vol. 03.01, West Conshohocken, PA, 2001, E647.

[39]Marchand, N., Parks, D. M., and Pelloux, R. M., "K_I Solutions for Single Edge Notch Specimens Under Fixed End Displacements," *International Journal of Fracture*, Vol. 31, 1986, pp. 53–65.

[40]Pang, C. M., and Song, J. H., "Crack Growth and Closure Behavior of Short Fatigue Cracks," *Engineering Fracture Mechanics*, Vol. 47, No. 3, 1994, pp. 327–343.

[41]Newman, J. C., Jr., Wu, X. R., Venneri, S. L., and Li, C. G., "Small Crack Effects in High-Strength Aluminum Alloys," NASA/CAE Cooperative Program, NASA RP-1309, NASA Langley Research Center, Hampton, VA, 1994.

[42]Lee, S. Y., and Song, J. H., "Crack Closure and Growth Behavior of Physically Short Fatigue Cracks Under Random Loading," *Engineering Fracture Mechanics*, Vol. 66, 2000, pp. 321–346.

S. Saigal
Associate Editor